

Trading with the Momentum Transformer: An Intelligent and Interpretable Architecture

Kieran Wood*, Sven Giegerich†, Stephen Roberts*, Stefan Zohren*

*Oxford-Man Institute of Quantitative Finance, University of Oxford

†Oxford Internet Institute, University of Oxford

17th December 2021

Abstract—Deep learning architectures, specifically *Deep Momentum Networks* (DMNs) [1], have been found to be an effective approach to momentum and mean-reversion trading. However, some of the key challenges in recent years involve learning long-term dependencies, degradation of performance when considering returns net of transaction costs and adapting to new market regimes, notably during the SARS-CoV-2 crisis. Attention mechanisms, or Transformer-based architectures, are a solution to such challenges because they allow the network to focus on significant time steps in the past and longer-term patterns. We introduce the *Momentum Transformer*, an attention-based architecture which outperforms the benchmarks, and is inherently interpretable, providing us with greater insights into our deep learning trading strategy. Our model is an extension to the LSTM-based DMN, which directly outputs position sizing by optimising the network on a risk-adjusted performance metric, such as Sharpe ratio. We find an attention-LSTM hybrid Decoder-Only Temporal Fusion Transformer (TFT) style architecture is the best performing model. In terms of interpretability, we observe remarkable structure in the attention patterns, with significant peaks of importance at momentum turning points. The time series is thus segmented into regimes and the model tends to focus on previous time-steps in alike regimes. We find changepoint detection (CPD) [2], another technique for responding to regime change, can complement multi-headed attention, especially when we run CPD at multiple timescales. Through the addition of an interpretable variable selection network, we observe how CPD helps our model to move away from trading predominantly on daily returns data. We note that the model can intelligently switch between, and blend, classical strategies – basing its decision on patterns in the data.

I. INTRODUCTION

Time-series momentum (TSMOM) strategies [3], also known as trend following or ‘follow the winner’ strategies, are based on the simple heuristic of going long (short) on assets with positive (negative) returns over some lookback window. It is an observed anomaly in asset prices, meaning it performs contrary to the notion of the Capital Asset Pricing Model (CAPM) [4]. It has been observed that stocks with larger relative returns over the past year tend to have higher average returns over the subsequent year [5], contradicting the efficient market hypothesis. The momentum effect has been widely studied [3, 6–8] and TSMOM strategies are a consistent component of managed futures or Commodity Trading Advisors (CTAs) [9]. The standard approach involves quantifying the magnitude of trends [8, 10, 11] and sizing traded positions accordingly [12–14]. The univariate TSMOM strategies we focus on differ to the cross-sectional approach [15] which studies the comparative performance of assets. This is achieved by ranking a portfolio of assets based on their relative historical performance, for example, buying the top decile of assets and selling the bottom decile at a given time step.

Deep Momentum Networks (DMNs) [1, 2] are a deep learning framework which can learn to size both the trend and position in a data driven manner by directly optimising on the Sharpe ratio of the signal, typically using a Long Short-Term Memory (LSTM) [16] architecture, significantly outperforming classical approaches from approximately 2003 on-wards, when electronic trading was becoming more prominent [2]. The LSTM, initially

*Kieran Wood is the corresponding author and can be contacted via email: kieran.wood@eng.ox.ac.uk.

proposed to address the vanishing and exploding gradient problem [17], is a special kind of Recurrent Neural Network (RNN) [18], which is a class of artificial neural networks models where information can flow from one step to another. In addition to exploiting long term trends, DMNs have also been observed to simultaneously exploit localised price fluctuations with a fast mean-reversion strategy [2]. Mean-reversion [19–21] strategies assume losers (winners) over some time horizon window will be winners (losers) in the subsequent period and are known as ‘follow the loser’ strategies.

We note that even DMNs have been underperforming in recent years, such as during the SARS-CoV-2 crisis, which can be attributed to the presence of nonstationarity or momentum turning points, where a trend breaks down [22]. Whilst the LSTM is good at learning local patterns [23], this architecture is known to struggle with long term patterns and responding to significant events, such as a market crash, which we term as regime change.

One proven approach to making an LSTM DMN model more robust to regime change, in a data-driven manner, is via the introduction of an online changepoint detection (CPD) [2] module to our DMN pipeline. The CPD module uses a principled Bayesian Gaussian Process [24] region switching approach [25], which is robust to noisy inputs, to detect regime change. Whilst this approach certainly helps to alleviate some of the issues, it can still place too much emphasis on the fast-reverting regime, resulting in poor performance when considering returns net of transaction cost. Furthermore, due to the nature of the architecture, the model is difficult to interpret.

In this paper, we introduce the *Momentum Transformer*, a subclass of DMNs which incorporates attention mechanisms [26]. An attention mechanism is a key-value lookup based on a given query. Initially proposed as a sequence-to-sequence [27] model, attention based Transformer [28] architectures have led to state-of-the-art performance in diverse fields, such as of natural language processing, computer vision, and speech processing [29]. Transformers employ self-attention which relates different positions of a sequence to compute some representation of the sequence.

Transformer architectures have been proven to

be effective for cross-sectional momentum strategies [30] and recently have been harnessed for time-series modelling [31–33]. Former work has predominantly focused on forecasting tasks which typically feature periodic components and a higher signal-to-noise ratio than financial time series. In the context of time-series, we prevent any points attending to future time-steps with a process known as masking. Attention mechanisms are known to lead to improvements in learning long term dependencies, with the ability to attend to significant events and learn regime specific temporal dynamics [23]. Whilst we observe the introduction of an attention mechanism to help respond to regime change, similarly to the inclusion of a CPD module, we observe that our architecture and a CPD module perform well together, leading to superior returns.

We find an attention-LSTM hybrid Decoder-Only Temporal Fusion Transformer (TFT) style architecture is the best performing model after benchmarking it against the canonical Transformer and a number of time-series forecasting specific architectures: the Decoder-Only Transformer, the Convolutional Transformer, and the Informer. All Transformer architectures we assess exhibit strong risk-adjusted returns during recent years such as the 2015–2020 period, where switching from an LSTM to a TFT architecture improves Sharpe ratio by 109%. All Transformer architectures lead to considerable profits in the SARS-CoV-2 crisis – in contrast, using an LSTM-based DMN during this crisis, leads to significant losses.

An important consideration when trading with DMNs is to understand why the model selects a given position. While [2] provides some insight into the concurrent slow momentum and fast reversion strategies, with regard to examining how the model adjusts its position sizing during different regimes, the original DMN model is largely a black box. Explanation methods such as LIME [34] and SHAP [35] can be applied post-hoc, providing insights into variable importance. However, these approaches fail to take into account time ordering. One of the innovations of the TFT [32] is that it is constructed using components which are inherently interpretable, with its Variable Selection Network naturally providing a measure of variable importance. It provides insight into how the model combines

different classical TSMOM and Moving Average Convergence Divergence (MACD) [8] strategies at different times. Furthermore, the attention patterns, which focus on previous time-steps, show significant structure and splits the time series into regimes. At a given time-step, the model focuses on alike regimes and places significant importance on momentum turning points.

II. BACKGROUND

A. Attention

The self-attention mechanism, which relates positions of a sequence to construct a representation, is at the core of all Transformer-based architectures assessed in this paper. There are numerous variations of computing attention [26, 36], however, similarly to [28], we use the Scaled Dot-Product,

$$\text{Att}(\mathbf{Q}, \mathbf{K}, \mathbf{V}) = \text{softmax}\left(\frac{\mathbf{Q}\mathbf{K}^\top}{\sqrt{d_{\text{model}}}}\mathbf{U}\right)\mathbf{V}, \quad (1)$$

which scales values $\mathbf{V} \in \mathbb{R}^{n \times d_v}$ for queries $\mathbf{Q} \in \mathbb{R}^{n \times d_{\text{att}}}$ and keys $\mathbf{K} \in \mathbb{R}^{n \times d_{\text{att}}}$. We denote the dimension of the embedding input as d_{model} , using the $(1/\sqrt{d_{\text{model}}})$ factor to mitigate issues caused by small gradients in the softmax operator. To avoid information leakage, we can include \mathbf{U} for masking, which sets all upper triangular values to $-\infty$, or alternatively \mathbf{U} is the identity matrix if no masking is required. As proposed in [28], we can expand this idea to multiple heads for different representation subspaces, resulting in improved learning capacity,

$$\text{MHA}(\mathbf{Q}, \mathbf{K}, \mathbf{V}) = [\text{head}_1, \dots, \text{head}_h] \mathbf{W}^{\mathbf{O}} \quad (2)$$

$$\text{head}_i = \text{Att}(\mathbf{Q}\mathbf{W}_i^{\mathbf{Q}}, \mathbf{K}\mathbf{W}_i^{\mathbf{K}}, \mathbf{V}\mathbf{W}_i^{\mathbf{V}}) \quad (3)$$

where each head_i (out of h heads) refers to the i th attention mechanism of Equation 1, and learned parameter matrices,

$$\begin{aligned} \mathbf{W}_i^{\mathbf{Q}} &\in \mathbb{R}^{d_{\text{model}} \times d_q}, & \mathbf{W}_i^{\mathbf{K}} &\in \mathbb{R}^{d_{\text{model}} \times d_k}, \\ \mathbf{W}_i^{\mathbf{V}} &\in \mathbb{R}^{d_{\text{model}} \times d_v}, & \mathbf{W}^{\mathbf{O}} &\in \mathbb{R}^{hd_v \times d_{\text{model}}}, \end{aligned}$$

where typically $d_q = d_k = d_v = d_{\text{model}}/h$. We apply self-attention as,

$$\mathbf{Y}(t) = \text{MHA}(\Theta(t), \Theta(t), \Theta(t)). \quad (4)$$

where $\Theta(t)$ is the embedding for prediction time t , allowing the inputs to interact with each other and

determine how much attention should be given to other time-steps.

It was proposed by [32], that we can share the value weights across heads, meaning each head can learn different temporal patterns while attending to a common set of input features. This is beneficial when interpreting the attention patterns and is referred to as Interpretable MHA (IMHA),

$$\text{IMHA}(\mathbf{Q}, \mathbf{K}, \mathbf{V}) = \tilde{\mathbf{H}}\mathbf{W}^{\mathbf{H}}, \quad (5)$$

$$\tilde{\mathbf{H}} = \frac{1}{h} \sum_1^{m_H} \text{Att}(\mathbf{Q}\mathbf{W}_i^{\mathbf{Q}}, \mathbf{K}\mathbf{W}_i^{\mathbf{K}}, \mathbf{V}\mathbf{W}^{\mathbf{V}}), \quad (6)$$

where $\mathbf{W}^{\mathbf{H}} \in \mathbb{R}^{d_{\text{att}} \times d_{\text{model}}}$ is a linear mapping and weight matrix $\mathbf{W}^{\mathbf{V}} \in \mathbb{R}^{d_{\text{model}} \times d_v}$ represents the attention weights shared across all heads.

B. Transformer

The canonical Transformer [28], an encoder-decoder architecture, was initially designed for sequence-to-sequence applications. The encoder maps input sequence \mathcal{Z} to an intermediate sequence of abstract representations, often called memory \mathcal{Y} . Passing this through the decoder produces an output sequence \mathcal{X} . Each side consists of multiple stacks of $l \in \{1, \dots, M\}$ identical layers. Each layer consists of a (multi) self-attention mechanism followed by a position-wise feed-forward network with dimension d_{hidden} , with a residual connection [37] between these two components. The model includes a dropout layer [38], and utilises layer normalisation.

It has been shown that the self-attention mechanism benefits from an embedding layer [28], which is the projection of the input, of size d_{input} , into a higher dimensional space of size d_{model} . While RNN models capture the positional time-series pattern via their recurrent structure, the Transformer needs to preserve the positional context explicitly because the dot-product operation cannot capture this local context. We must inject some information about the relative or absolute position of the sequence items, which we add to the embedding. Positional encoding can either be fixed or learnable, however, we find that there is little difference in the results in the context of momentum trading and it increases the number of model parameters unnecessarily. In this paper we use the standard positional encoding and we enrich the embedding with asset static information. In line

with [33], we add a timestamp through learnable year and month embeddings. In general, it would also be possible to include an even finer timestamp granularity such as weeks or days.

It has been demonstrated by [31] that the decoder side of the transformer architecture can be sufficient for time series forecasting however it is argued by [33] that Transformers are inherently designed as an encoder-decoder architecture and illustrated that a vanilla encoder-decoder Transformer is superior to a Decoder-Only Transformers. In this paper we assess both of these variants of the Transformer.

C. Convolutional Transformer

The Convolutional Transformer [31] incorporates convolutional and log-sparse self-attention in order to increase the Decoder-Only Transformer’s awareness of locality as well as decreasing the quadratic memory cost of the attention-mechanism. It addresses the possibility that a single point in time might be very much dependent on the surrounding context, or patterns. This is achieved by adding a causal convolution operation, before the self-attention query-key input, of kernel size k and stride 1, with $k = 1$ being the standard self-attention. An initial motivation was shopping patterns around holidays, however this concept fits in neatly with the concept of market regimes. Further, it was observed that the canonical self-attention mechanism often attributes very little attention to most keys, focusing only on few important keys. The authors, therefore, proposed *LogSparse* attention setting many attention keys statically to zero (inactive). Specifically, each cell is only permitted to attend to its previous cells with exponential step size and itself, which restricts the number of parameters, or keys, immensely.

D. Informer

The Informer, proposed by [33], replaces the naive sparsity rule with a measurement based on the Kullback-Leibler divergence [39] to distinguish essential queries, referred to as *ProbSparse* self-attention. The model has approximately the same parameter space as the Convolutional Transformer, but the attention mechanism computes the difference between the distance of the self-attention distribution and the naive uniform distribution content-based. If there is substantial distance, the query is set active,

otherwise it is treated as inactive. Furthermore, the model decreases the dimension d_{model} by half for each layer to further reduce the parameter space, which is a process termed as ‘distilling’.

E. Temporal Fusion Transformer

The TFT [32] is constructed by piecing together a number of intelligent components, each with their own function, as an input. In its original guise, it is an encoder-decoder architecture, however, for the *Momentum Transformer* we propose a Decoder-Only variation. We borrow a number of the TFT components, including IMHA which we have previously detailed.

LSTM Encoder: Whilst [28] proposes ‘attention is all you need’, doing away with convolutions and RNNs, [32] suggests that it can still be beneficial to deal with positional encoding via an LSTM encoder for time-series applications. The TFT is, an attention-LSTM hybrid model which uses recurrent LSTM layers for local processing and interpretable self-attention layers for long-term dependencies.

Static variables: The TFT supports static covariates, where Entity Embeddings [40] are used as feature representations for categorical variables, and linear transformations for continuous variables. In the context of the *Momentum Transformer*, we include the asset type, however there is the possibility to include other covariates here.

Gated Linear Unit (GLU): The GLU [41] is a component which we use to suppress any component which makes the architecture overly complex. For input \mathbf{x}_d , which Dropout [38] has been applied to,

$$\text{GLU}(\mathbf{x}_d; \theta_1, \theta_2) = (\mathbf{W}_1 \mathbf{x}_d + \mathbf{b}_1) \odot \sigma(\mathbf{W}_2 \mathbf{x}_d + \mathbf{b}_2), \quad (7)$$

with \odot being the element-wise Hadamard product, $\sigma(\cdot)$ the sigmoid activation function, $\mathbf{W}_{(\cdot)} \in \mathbb{R}^{d_{\text{model}} \times d_{\text{model}}}$ learnable weights and $\mathbf{b}_{(\cdot)} \in \mathbb{R}$ learnable biases. This is followed by an *Add and Norm* component which adds the activation of the GLU with the output of a previous component (the skip connection), then normalise this to have zero mean and unit standard deviation.

Gated Residual Networks for optional non-linear processing: The *Gated Residual Network* (GRN), proposed by [32], is a building block which applies non-linear processing, but only when required, to

make our model more robust. In the case where we have a small or noisy dataset, this component defaults to a simpler linear model, with the key component being the Exponential Linear Unit (ELU) which can either act as a linear or nonlinear layer. It is both preceded and followed by a dense layer. There is the ability to skip the building block via a GLU followed by an *Add & Norm*. Optionally, this component can have an additional static context input to the first dense layer.

Variable Selection Network: This sample-dependent component is used to select the variables which are of most significance for the prediction problem, filtering out any inputs with a low signal rate. The Variable Selection Network is applied to both static covariates and time-dependent covariates. Processed features $\tilde{\xi}_{t,j}$ are weighted by their variable selection weights $\eta_{t,j}$ and combined as,

$$\tilde{\xi}_t = \sum_{j=1}^m \eta_{t,j} \tilde{\xi}_{t,j}, \quad (8)$$

where j indicates the covariate. Full details of the implementation can be found in [32].

F. Changepoint Detection Module

The CPD module is a preprocessing step, where we run online changepoint detection on the daily returns data. We find a single changepoint for a pre-defined lookback window length (LBW). For every time-step, our CPD module pre-computes two normalised features,

- 1) changepoint detection location $\gamma_t^{(i)} \in (0, 1)$, indicating how far in the past the changepoint is, and
- 2) changepoint score $\nu_t^{(i)} \in (0, 1)$, which captures the level of disequilibrium, measured by the reduction in negative log marginal likelihood achieved via the introduction of the changepoint kernel hyperparameters.

Details of the implementation can be found in [2].

III. MOMENTUM TRANSFORMER

For all Transformer architectures tested, we adhere to the *Deep Momentum Network* (DMN) framework [1]. An important part of this framework is volatility scaling [14, 12], where we scale the returns of each asset by its volatility, so that each asset has a similar

contribution to the overall portfolio returns. We target a consistent annualised volatility σ_{tgt} , which we choose to be 15% for consistency with previous works [1, 2]. The realised return of our strategy from day t to $t+1$ is,

$$R_{t+1}^{\text{TSMOM}} = \frac{1}{N} \sum_{i=1}^N R_{t+1}^{(i)}, \quad R_{t+1}^{(i)} = X_t^{(i)} \frac{\sigma_{\text{tgt}}}{\sigma_t^{(i)}} r_{t+1}^{(i)}, \quad (9)$$

where N is the number of assets. For the i -th asset, $X_t^{(i)}$ is our position size and $\sigma_t^{(i)}$ the ex-ante volatility, calculated using a 60-day exponentially weighted moving standard deviation.

The DMN framework involves simultaneously learning both trend and sizing a position accordingly as,

$$\mathbf{X}_{T-\tau+1:T}^{(i)} = (\tanh \circ f \circ g) \left(\mathbf{u}_{T-\tau+1:T}^{(i)} \right), \quad (10)$$

where τ is our sequence length, $g(\cdot)$ is our candidate machine learning architecture and $f(\cdot)$ a time distributed, fully-connected layer, followed by an element-wise tanh activation function. For each time-step in the sequence, this maps next-day position as $X_t^{(i)} \in (-1, 1)$, where $X_t^{(i)} = 1$ indicates a maximum long position and $X_t^{(i)} = -1$ a maximum short position. We train via mini-batch Stochastic Gradient Descent (SGD) using the *Adam* [42] optimiser, with loss function selected to directly maximise some risk-adjusted metric, which for the Sharpe ratio involves minimising,

$$\mathcal{L}_{\text{sharpe}}(\boldsymbol{\theta}) = -\frac{\sqrt{252} \mathbb{E}_{\Omega} \left[R_t^{(i)} \right]}{\sqrt{\text{Var}_{\Omega} \left[R_t^{(i)} \right]}}, \quad (11)$$

where Ω contains all asset-time pairs in the mini-batch.

We focus on the details of our best performing architecture, the *Momentum Transformer*, a Decoder-Only TFT DMN, and provide a schematic of the architecture in Exhibit 1. For other reference architectures we simply substitute $g(\cdot)$ in (10) with the chosen architecture and details can be found in Appendix B.

Our input features include returns at different timescales, which are normalised using ex-ante volatility $\sigma_t^{(i)}$, corresponding to daily, monthly, quarterly, biannual and annual returns. We also use

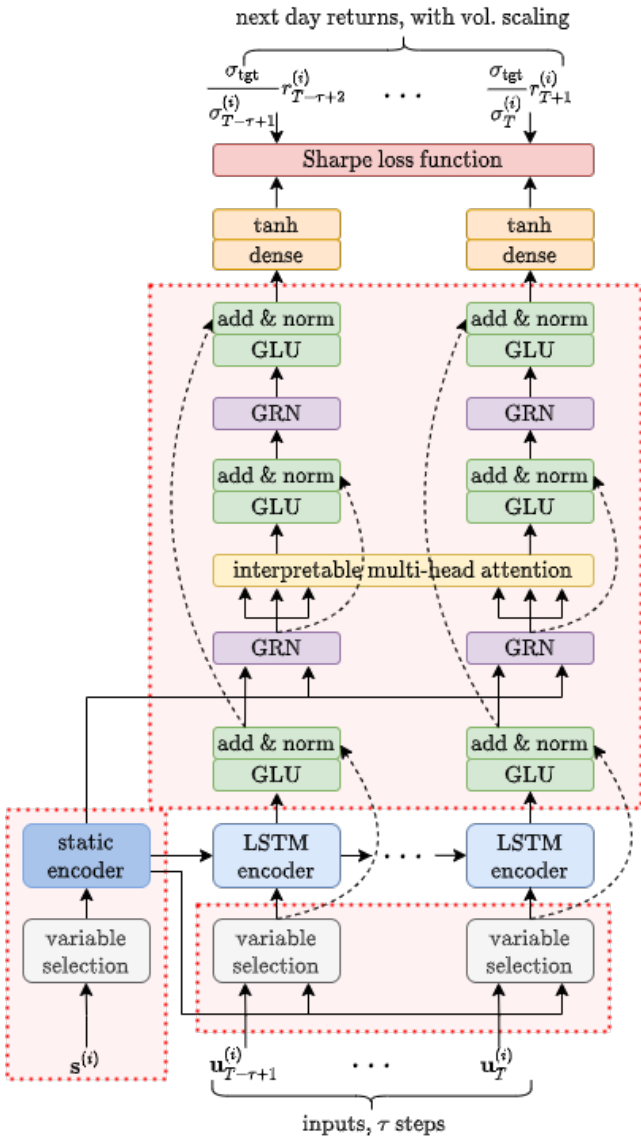


Exhibit 1: Momentum Transformer architecture. The dotted red boxes indicate the additional components we are adding to the LSTM-based DMN architecture. Details of the TFT components can be found in [32].

MACD [8] indicators which are a volatility normalised moving average convergence divergence indicator $M_t^{(i)}(S, L)$, defining the relationship between a short S and long signal L . The implementation of MACD indicators in DMNs is detailed in [1]. Finally we optionally pass CPD location $\gamma_t^{(i)}(l)$ and severity $\nu_t^{(i)}(l)$ parameters across different timescales l [2], where a single changepoint is assumed in each look-back window. Multiple CPD timescales are enabled

by the Variable Selection Network component of the TFT, which removes any unnecessary inputs which negatively impact performance. At longer timescales the CPD module focuses on larger, more significant events and at shorter timescales, our model can detect events more rapidly or exploit more localised fluctuations. We report results for the *Momentum Transformer* with and without CPD. We do this as CPD has only previously been proven to be successful for an LSTM-based DMN and, additionally, we would like to observe how well the *Momentum Transformer* responds to regime change without CPD.

We summarise our model features \mathbf{u}_t for each time-step as,

- $\left\{ r_{t-t',t}^{(i)} / \sigma_t^{(i)} \sqrt{t'} \mid t' \in \{1, 21, 63, 126, 252\} \right\}$,
- $\left\{ M_t^{(i)}(S, L) \mid (S, L) \in \{(8, 24), (16, 28), (32, 96)\} \right\}$,
- $\left\{ \nu_t^{(i)}(l), \gamma_t^{(i)}(l) \mid t' \in \{21, 126\} \right\}$, if the CPD module is used.

In the case of the Decoder-Only TFT we have a static variable input,

$$\mathbf{s}^{(i)} = [\text{asset}^{(i)}], \quad (12)$$

which is a single categorical variable, encoding information for the asset-class.

For the other benchmark Transformer architectures, we construct our embedding as a sum of four separate parts 1) a scalar projection, from d_{input} to d_{model} , 2) the asset’s entity embedding [40], 3) the local context, i.e., the timestamp, and 4) learnable year and month embeddings.

IV. BACK-TESTING DETAILS

For all of our experiments, we used a portfolio of 50 of the most liquid, continuous futures contracts over the period 1990–2020, extracted from the Pinnacle Data Corp CLC Database [43]. It is a balanced portfolio consisting of commodities, equities, fixed income and FX futures. This dataset has been previously used to benchmark strategies [2, 44] and further details of the dataset can be found in Appendix A. We use an expanding window approach, where we initially use 1990–1995 for training-validation, then test out-of-sample on the period 1995–2000, expand the training-validation set to 1990–2000, test out-of-sample on the subsequent

five years, and so on. We present results for three different scenarios:

- 1) **Average test results over all five year windows 1995–2020**, allowing us to measure performance over a sustained period and additionally capture how effective the architecture is early on, when limited data is available.
- 2) **Test results over the period 2015–2020**, which provides insight into how our candidates perform across recent years which exhibited significant nonstationarity. In this time period both classical strategies and LSTM-based DMNs have been observed to under-perform, however CPD has previously been observed to somewhat alleviate this degradation [2].
- 3) **The SARS-CoV-2 crisis**, from 1 January 2020 until 15 October 2020, to observe how our candidate architectures deals with regime change, including the market crash and the subsequent Bull market.

Our *Momentum Transformer* candidate architectures correspond to $g(\cdot)$ in Equation (10) and were chosen as: 1) Transformer, 2) Decoder-Only Transformer, 3) Convolutional Transformer, 4) Informer, and 5) Decoder-Only TFT. Additionally, we tested a variation of the best performing architecture, the Decoder-Only TFT, where we included CPD covariates. All details of the experiments can be found in Appendix B and for additional details, please refer to [1, 2]. Architecture hyper-parameters were tuned with Random Grid Search, using the validation set diversified portfolio Sharpe ratio as loss function. This process is also detailed in Appendix B.

V. RESULTS AND DISCUSSION

A. Performance

We have recorded the results, for each of our three testing scenarios, in Exhibit 2. We consider,

- 1) **profitability** through annualised returns and percentage of positive captured returns,
- 2) **risk** through annualised volatility, annualised downside deviation and maximum drawdown (MDD), and
- 3) **risk-adjusted performance** through annualised Sharpe, Sortino and Calmar ratios.

Since we completely rerun each experiment five times, we have reported the average across all runs, for each metric. The Decoder-Only TFT outperforms the benchmark architectures across all risk-adjusted performance metrics for scenarios 1 and 2. Notably, compared to the LSTM, Sharpe ratio is improved by 50% during the period 1995–2020 and during 2015–2020 the improvement is 109%. In general, compared to the LSTM across all experiments, the *Momentum Transformer* has higher returns, predicts the direction of price more often and reduces all risk metrics overall. Whilst a lookback of approximately one annual quarter has previously been found to be optimal for LSTM-based DMNs, we note that the *Momentum Transformer* is able to learn longer-term patterns and works better with an input sequence length of one year.

We demonstrate that the addition of a CPD module can be complementary, rather than an alternative to multi-head attention, and in the period 2015–2020 we observe a further improvement in Sharpe ratio of 17% for the *Momentum Transformer*. Furthermore, we demonstrated that it can be beneficial to input both a short LBW of one month and a longer LBW of half a year, allowing the Variable Selection Network to determine when these inputs are relevant in a data-driven manner.

Whilst the other transformer architectures do not perform as well as the Decoder-Only TFT in the first two experiments, Exhibit 3 reveals that there is a clear upward trend in recent years, during which the performance of the other non-hybrid Transformer architectures is comparable to the TFT. During the SARS-CoV-2 crisis the Transformer (canonical and Decoder-Only), and the Informer outperform even the Decoder-Only TFT. This period of clearly defined regimes, with a large crash followed by a Bull market, is unsurprisingly home turf for attention based architectures. The LSTM exhibits very poor performance during this experiment and we argue that the LSTM is better suited to exploiting short term patterns. In contrast, the LSTM still performs reasonably well during the 2008 financial crisis. This is likely because there was more signal in the lead up to this event, compared to the SAR-CoV-2 crash which was sudden and caused by exogenous factors. Being an attention-LTSM hybrid, the TFT model tends to be more of an all-rounder, with a more stable

Exhibit 2: Strategy Performance Benchmark – Raw Signal Output.

	Returns	Vol.	Sharpe	Downside Deviation	Sortino	MDD	Calmar	% of +ve Returns	Ave. P Ave. L
Average 1995–2020									
Long-Only	2.45%	4.95%	0.51	3.51%	0.73	12.51%	0.21	52.43%	0.988
TSMOM	4.43%	4.47%	1.03	3.11%	1.51	6.34%	0.94	54.23%	1.002
LSTM	2.71%	1.67%	1.70	1.10%	2.66	2.14%	1.68	55.17%	1.091
Transformer	3.14%	2.49%	1.41	1.68%	2.13	2.92%	1.53	54.71%	1.051
Decoder-Only Trans.	2.95%	2.61%	1.11	1.74%	1.69	3.47%	1.09	53.50%	1.051
Conv. Transformer	2.94%	2.75%	1.07	1.87%	1.60	3.80%	0.98	53.55%	1.041
Informer	2.39%	1.38%	1.72	0.89%	2.67	1.43%	1.79	54.88%	1.103
Decoder-Only TFT	4.01%	1.54%	2.54	0.96%	4.14	1.32%	3.22	57.34%	1.154
Decoder-Only TFT CPD	3.70%	1.37%	2.62	0.85%	4.25	1.29%	3.22	57.66%	1.151
Average 2015–2020									
Long-Only	1.73%	5.00%	0.37	3.59%	0.51	11.41%	0.15	51.97%	0.982
TSMOM	0.97%	4.38%	0.24	3.19%	0.33	8.25%	0.12	52.82%	0.931
LSTM	1.23%	1.85%	0.82	1.32%	1.19	3.55%	0.66	53.38%	1.004
Transformer	1.98%	1.29%	1.53	0.85%	2.32	1.07%	1.86	54.76%	1.071
Decoder-Only Trans.	1.37%	1.97%	0.72	1.37%	1.03	2.63%	0.60	52.76%	1.012
Conv. Transformer	1.85%	1.92%	0.98	1.30%	1.47	3.14%	0.77	52.93%	1.056
Informer	1.67%	1.09%	1.51	0.72%	2.30	1.17%	1.44	54.39%	1.089
Decoder-Only TFT	1.99%	1.23%	1.71	0.82%	2.61	1.17%	2.06	55.72%	1.073
Decoder-Only TFT CPD	2.06%	1.02%	2.00	0.66%	3.10	0.82%	2.53	55.74%	1.120
SARS-CoV-2									
Long-Only	-1.46%	6.73%	-0.19	5.64%	-0.22	12.32%	-0.12	57.28%	0.720
TSMOM	0.90%	4.73%	0.21	3.14%	0.32	4.17%	0.22	50.00%	1.041
LSTM	-4.15%	2.82%	-1.50	2.52%	-1.67	5.35%	-0.78	52.29%	0.643
Transformer	4.42%	1.28%	3.38	0.83%	5.55	0.84%	7.31	64.85%	1.066
Decoder-Only Trans.	8.02%	2.58%	3.01	1.42%	5.55	1.05%	8.56	58.83%	1.243
Conv. Transformer	3.13%	1.99%	1.81	1.40%	2.74	1.61%	3.17	57.48%	1.058
Informer	4.30%	1.60%	2.71	1.00%	4.45	1.07%	4.28	59.61%	1.137
Decoder-Only TFT	1.81%	1.75%	1.22	1.37%	1.74	2.14%	1.57	60.39%	0.831
Decoder-Only TFT CPD	3.39%	1.51%	2.47	1.03%	4.08	1.15%	5.92	59.90%	1.068

average Sharpe ratio across all years. It should be noted that we observe slightly more variance in the repeats of experiments for the TFT, which is likely attributed to the fact that the TFT is a more complex architecture and hence more sensitive to the tunable hyperparameters.

Interestingly, the canonical Transformer outperforms the Informer during the SARS-CoV-2 crisis and over the 2015–2020 period. While the Informer has proven to produce superior results for other applications [33], it is thus not necessarily the most suitable architecture for momentum trading. This could be because the Informer is designed for time-series which exhibit stronger periodicity or a setting with a higher signal-to-noise ratio in general. Similarly, the Convolutional Transformer does not outperform the Decoder-Only Transformer, again highlighting the challenges of attending to localised

patterns in a low signal-to-noise setting.

We provide plots of returns for experiment scenarios 2 and 3 in Exhibit 4. These plots further illustrate how the LSTM is unsuitable during the market nonstationarity of 2015–2020 and during the SARS-CoV-2 crisis. Whilst the Transformer architectures are all able to respond naturally to sudden regime change, especially in comparison to the LSTM, we do observe that the addition of the CPD module still significantly helps with the timing of this response. It is evident that the non-hybrid Transformer models perform exceptionally well once the Bull market is established after the SARS-CoV-2 market crash, exploiting this regime with slow momentum.

B. Interpretability

Not only is the TFT-based architecture the best performing, but it also has additional benefits of be-

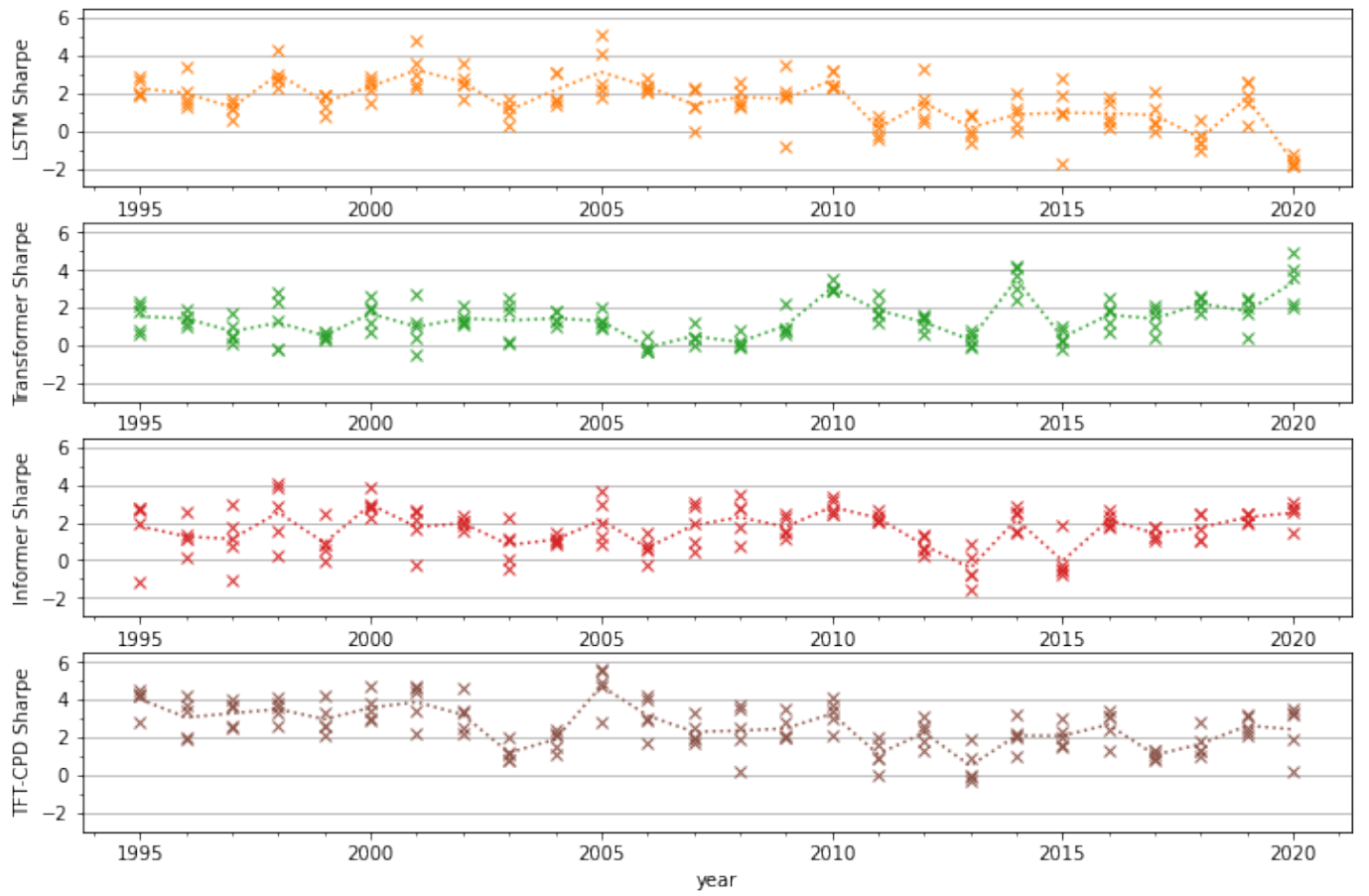


Exhibit 3: Average annual Sharpe ratio by year, including the results for each of the five experiment repeats.

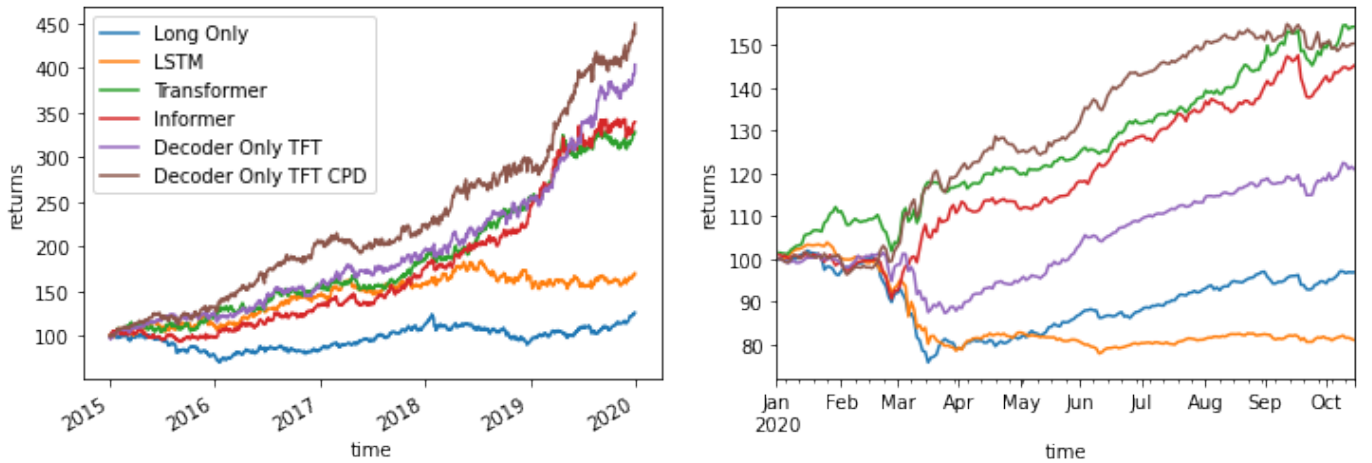


Exhibit 4: These plots benchmark our strategy performance for the 2015–2020 scenario (left) and the SARS-CoV-2 scenario (right). For each plot we start with \$100 and we re-scale returns to 15% volatility. Since we ran each experiment five times, we plot the repeat which resulted in the median Sharpe ratio, across the entire experiment.

Exhibit 5: Decoder-Only TFT average variable importance.

	2015–2020		SARS-CoV-2	
	no CPD	with CPD	no CPD	with CPD
\hat{r}_{day}	30.8%	23.3%	24.4%	21.2%
\hat{r}_{month}	13.6%	5.7%	10.6%	7.4%
\hat{r}_{quarter}	8.9%	7.4%	14.0%	5.7%
$\hat{r}_{\text{biannual}}$	8.9%	6.2%	8.5%	7.5%
\hat{r}_{annual}	11.9%	10.5%	13.5%	8.8%
$M_t^{(i)}(8, 24)$	9.1%	7.3%	9.7%	12.9%
$M_t^{(i)}(16, 48)$	10.3%	6.6%	11.9%	6.3%
$M_t^{(i)}(32, 98)$	6.5%	5.7%	7.3%	8.7%
CPD Score 21	-	6.4%	-	4.1%
CPD LBW 21	-	7.0%	-	7.6%
CPD Score 126	-	4.7%	-	4.8%
CPD LBW 126	-	9.2%	-	4.9%

ing more interpretable. We analyse two components, both of which are detailed in [32],

- 1) **variable importance**, demonstrating how different classical strategies are blended at different times, in addition to their interaction with features from the CPD module, and
- 2) **interpretable multi-head attention**, providing insight into how our model focuses on significant events and similar regimes.

In Exhibit 5 we tabulate the variable importance for the Decoder-Only TFT, averaged across 2015–2020 and then for the SARS-CoV-2 crisis. We record results for the models, with and without CPD, averaged over all repeats of the experiment. Overall, we note that the daily return feature is allocated the highest weighting, however this is somewhat reduced after the addition of CPD. This suggests that the model is relying less on fast reversion and, with a total weighting of 27% allocated to the CPD features, it is apparent that the model is exploiting the CPD information. Interestingly CPD LBW length tends to be of greater importance than the score, indicating that the model is learning from patterns in this length metric. After the addition of CPD, the model relies less on return timescales other than the shortest (daily) and the longest (annual) timescale.

Comparatively, daily data information is less important during the SARS-CoV-2 crisis than the 2015–2020 period. This is likely because 2015–2020 is a highly non-stationary period, however 2020 is characterised by a large crash followed by a clear

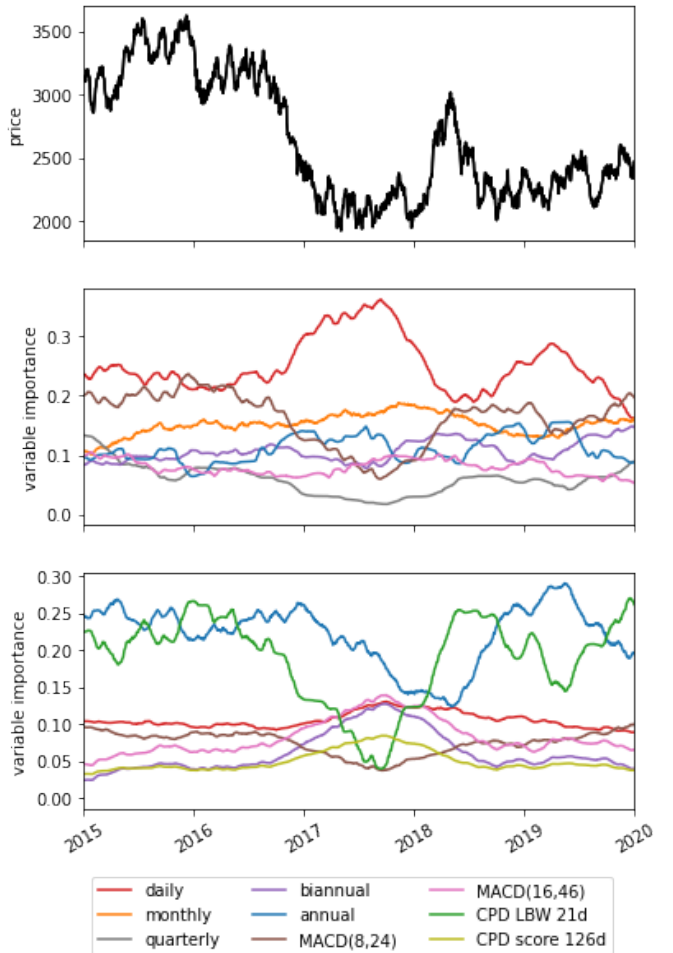


Exhibit 6: Variable importance for Cocoa future, forecasting out-of-sample over the period 2015–2020. The middle plot is the Decoder-Only TFT and the bottom plot is the Decoder-Only TFT with CPD. For each model, we only plot the seven features with the highest average weighting. We plot Cocoa because it exhibits typical behaviour of the model trading a commodity future and is comprised of a series of clearly defined regimes during this period.

uptrend. During this period quarterly returns are given much more weighting, in the lack of CPD. Across the board, the MACD indicators are allocated above average importance, tweaking the importance of each depending on the scenario and whether it has access to CPD information. Interestingly, Exhibit 5 shows that CPD features are not given a high importance during the SARS-CoV-2 experiment, despite their inclusion doubling the Sharpe ratio. This could be attributed to the fact that the feature

is important for the crash, but then less important once a trend is established.

In Exhibit 6 we can see how the variable importance for trading on Cocoa futures changes over time, where our model intelligently blends different strategies at different points in time. In the lack of CPD, we observe the model take an approach where a number of strategies are blended, in this case initially with significant weighing on the MACD $M_t^{(i)}(8, 24)$ indicator and some weighting on monthly returns throughout the entire five year period. Once the price drops in about mid 2016, significant importance is allocated to daily returns. The model continues to place high importance on daily returns as it is entering a mean-reverting regime, however once the price starts to rise again near the start of 2018, we shift back towards the original strategy. Once the price crashes for a second time, and we move back into a mean-reverting regime, daily returns become more important again. If the CPD features are added, the model adopts an entirely different strategy where it primarily uses knowledge from the 21 day CPD module to trade in conjunction with annual returns, shifting to returns with shorter timescales after any momentum turning points.

The self-attention plots in Exhibits 7 and 8 both illustrate significant structure. Exhibit 7 demonstrates that greater attention is placed on similar regimes. Here two points in similar regimes, where there is a clear upward trend, have almost an identical pattern, only deviating from each other at the furthest time-steps. On the other hand, the attention pattern for a point inside a clear downward trend focuses more on other downward trends, and increases (decreases) its attention pattern when the other plots are decreasing (increasing). Approximately two-thirds along the plot, there appears to be some sort of stationary regime, where the opposing patterns stay approximately constant. Interestingly, the attention patterns tend to place significant attention on relevant momentum tuning points, partitioning the time-series into regimes and indicating that this is taken into account when selecting a strategy.

Structure in the attention pattern is further demonstrated during the SARS-CoV-2 crisis, in Exhibit 8, where our model recognises fundamental change caused by some exogenous factors. In this example, the peaks indicating momentum turning points are

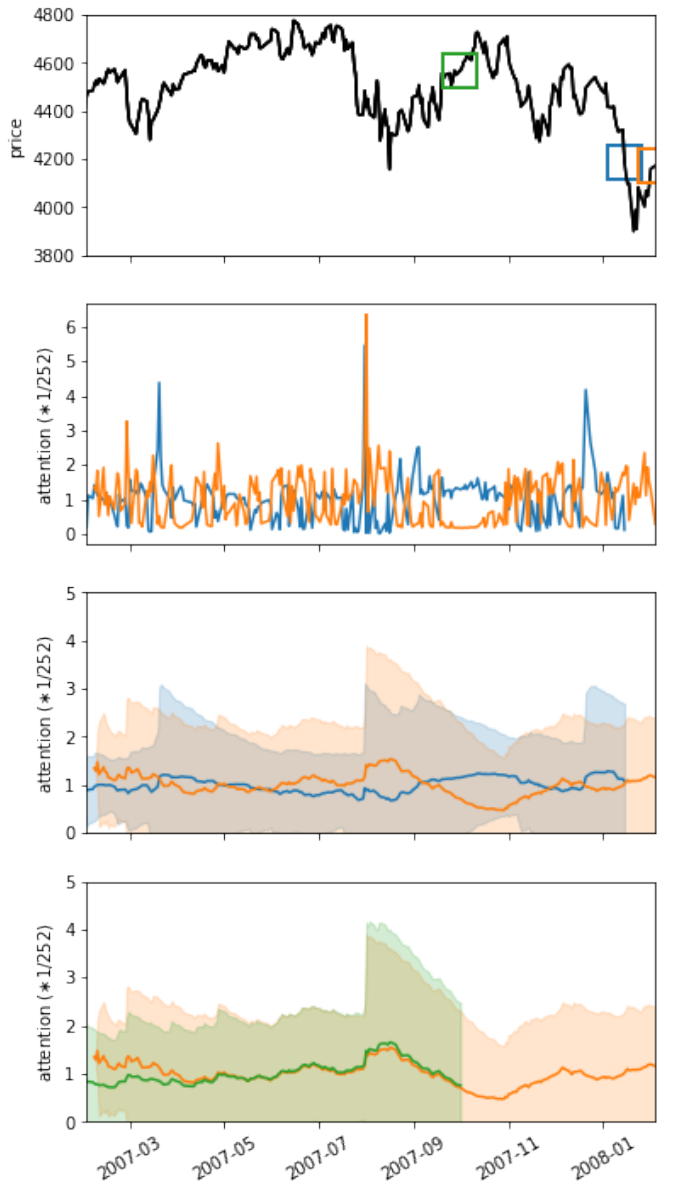


Exhibit 7: We plot the attention pattern for a single run of our Decoder-Only TFT CPD model, forecasting out-of-sample on FTSE 100 data in the lead up to the 2008 financial crash. We plot the patterns for 1 October 2007 (green), 15 January 2008 (blue), and 2 April 2008 (orange). In each case we are running the model for the next day, therefore, the plots all correspond to the last row of the weights matrix. The third and fourth plots show the 21 day exponentially weighted rolling average and standard deviations, with the shaded area representing the 95%-ile (± 1.96 standard deviations). These plots indicate how attention patterns are similar for points in the same type of regime, but oppose each other for different regimes.

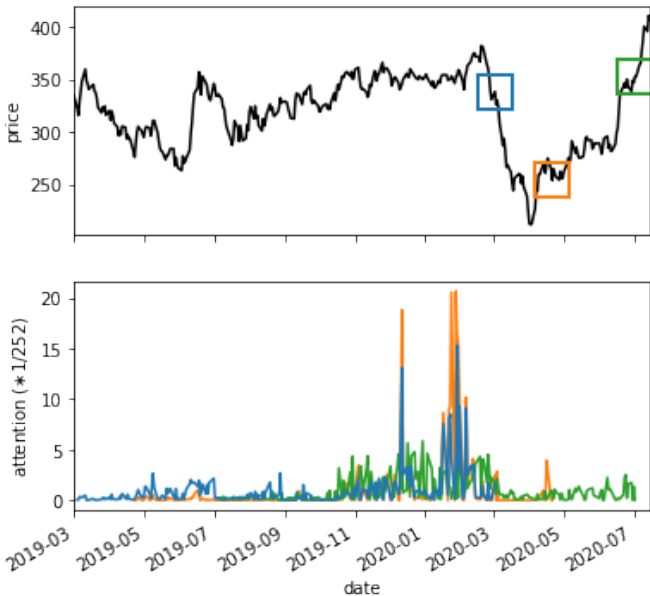


Exhibit 8: Lumber future price during SARS-CoV-2 crisis and the associated attention pattern when making a prediction at 1 March 2020 (blue), 21 April 2020 (orange), and 2 July 2020 (green), indicating that significant attention is placed on momentum turning points. We plot this future because it is characterised by a sudden crash caused by exogenous factors, immediately followed by a skyrocketing price.

even more pronounced, clearly segmenting the plot into regimes. This highlights the significance our model places on momentum turning points when selecting a strategy. Again, different turning points, are of greater importance depending on the point of reference.

C. Results Net of Transaction Costs

One of the weaknesses of DMNs is the performance net of transaction costs. This degradation is particularly acute in periods such as 2015–2020 where the model relies heavily on fast reversion.

In Exhibit 9 we detail the impact of transaction costs on the key architectures which we tested over 2015–2020. We increase the average cost C from 0bps to 3bps, to give returns,

$$\bar{R}_{t+1}^{(i)} = R_{t+1}^{(i)} + -C\sigma_{\text{tgt}} \left| \frac{X_t^{(i)}}{\sigma_t^{(i)}} - \frac{X_{t-1}^{(i)}}{\sigma_{t-1}^{(i)}} \right|. \quad (13)$$

It is important to note that we still train the model on raw returns, however for a proper treatment of transaction costs we can directly account for this in the loss function with a turnover regulariser, as demonstrated in [1].

We detail results by asset class, providing insight into the relative strengths and weaknesses of each architecture. Since there are more commodity futures in the portfolio, we look at the average Sharpe ratio for individual assets to ensure that we do not favour commodities which benefit more from diversification. When moving from raw returns to $C = 3\text{bps}$, the LSTM experiences a total reduction of 228%, whereas the Transformer is impacted the least and experiences a reduction of 106%. This suggests that attention based architectures focus more on long term trends and therefore are less impacted by transaction costs. The Decoder-Only TFT also performs exceptionally well net of transaction costs, with a Sharpe ratio of 1.22 for $C = 1\text{bps}$ when using a CPD module. The Transformer does outperform this architecture from $C = 2\text{bps}$ onwards, which could be attributed to the fact that the TFT favours fast reversion more due to the LSTM component. Alternatively, this could also be because it has been optimised for $C = 0\text{bps}$ and it was not focusing on transaction costs.

It can be noted that the LSTM performs well on equities and reasonably well on FX futures, which is likely due to its ability to learn localised patterns. The Transformer and Informer, on the other hand, perform well on the asset classes where it can identify longer trends, however, they perform poorly on FX where they need to be quicker. The Decoder-Only TFT gives the most rounded performance, performing very well across all asset classes, benefiting from both its LSTM and self-attention components. The addition of the CPD module has the biggest impact on commodities, where timing is particularly important. This translates to a superior portfolio performance, of which commodity futures is the biggest component. It should be noted that even at $C = 3\text{bps}$ the model performs very well on commodities. The relatively weak performance on Fixed Income across all architectures could be attributed to the fact that the portfolio is light on Fixed Income futures and is not given much weighting during the training process.

Exhibit 9: Transaction cost impact on Sharpe Ratio over 2015–2020 for individual assets, averaged by asset class, and for the entire diversified portfolio.

C	0bps	0.5bps	1bps	1.5bps	2bps	2.5bps	3bps
LSTM							
Indv. CM	0.12	0.09	0.05	0.01	-0.02	-0.06	-0.10
Indv. EQ	0.37	0.32	0.27	0.22	0.16	0.11	0.06
Indv. FI	0.09	-0.11	-0.32	-0.53	-0.74	-0.94	-1.15
Indv. FX	0.11	0.01	-0.08	-0.18	-0.27	-0.37	-0.46
Portfolio	0.82	0.51	0.20	-0.12	-0.43	-0.74	-1.05
Transformer							
Indv. CM	0.27	0.23	0.19	0.15	0.11	0.08	0.04
Indv. EQ	0.37	0.33	0.28	0.23	0.19	0.14	0.10
Indv. FI	0.23	0.03	-0.16	-0.35	-0.55	-0.74	-0.93
Indv. FX	-0.17	-0.24	-0.32	-0.39	-0.47	-0.55	-0.62
Portfolio	1.53	1.26	0.99	0.72	0.45	0.18	-0.09
Informer							
Indv. CM	0.28	0.24	0.19	0.15	0.10	0.06	0.01
Indv. EQ	0.34	0.28	0.22	0.16	0.10	0.04	-0.02
Indv. FI	0.08	-0.13	-0.35	-0.56	-0.78	-0.99	-1.20
Indv. FX	-0.14	-0.24	-0.33	-0.43	-0.53	-0.62	-0.72
Portfolio	1.51	1.17	0.83	0.49	0.15	-0.19	-0.53
Decoder-Only TFT							
Indv. CM	0.44	0.40	0.35	0.31	0.26	0.22	0.17
Indv. EQ	0.25	0.19	0.13	0.07	0.02	-0.04	-0.10
Indv. FI	0.30	0.05	-0.20	-0.45	-0.69	-0.94	-1.18
Indv. FX	0.28	0.18	0.08	-0.02	-0.12	-0.22	-0.32
Portfolio	1.71	1.36	1.01	0.67	0.32	-0.03	-0.37
Decoder-Only TFT CPD							
Indv. CM	0.55	0.50	0.45	0.40	0.35	0.30	0.25
Indv. EQ	0.18	0.12	0.05	-0.01	-0.07	-0.14	-0.20
Indv. FI	0.23	-0.03	-0.29	-0.55	-0.81	-1.07	-1.33
Indv. FX	0.24	0.13	0.02	-0.09	-0.20	-0.30	-0.41
Portfolio	2.00	1.61	1.22	0.83	0.44	0.04	-0.35

VI. CONCLUSIONS

We have demonstrated that our attention-based model, the *Momentum Transformer*, significantly outperforms the LSTM based *Deep Momentum Network* (DMN), across all risk-adjusted performance metrics. We have illustrated the suitability of the *Momentum Transformer* by back-testing over a sustained period of time from 1995–2020 and noting its comparatively strong performance in recent years. Our model is able to learn longer term patterns than the LSTM, benefiting from a longer input sequence length, specifically one year. Furthermore, all attention-based architectures, which we tested, are robust to significant events, such as during the SARS-CoV-2 market crash. Whilst an attention-LSTM hybrid Decoder-Only Temporal Fusion Transformer (TFT) model was the overall best performer, it can be noted

that results from the non-hybrid architectures, such as the Transformer and Informer, are on an upward trend in recent years and actually outperformed the TFT model during the SARS-CoV-2 market crash. Nonetheless, we propose the TFT model because it is arguably more robust, performing well more broadly. However, due to the comparative strengths of each model depending on the asset class and regime, we suggest it could be worthwhile to use an ensembling approach, where multiple learning algorithms are utilised to obtain better predictive performance, if trading in practice.

Our detailed study of the results by asset class demonstrate that the *Momentum Transformer* performs exceptionally well even net of costs. If we were to trade only with the 25 commodity futures in the period 2015–2020, we would still achieve a

portfolio Sharpe ratio of 1.23 at average transaction cost $C = 3$ bps. The reasoning for this could simply be because our portfolio contains more commodities than other asset classes, skewing its performance. It could be worthwhile to employ a transfer learning approach where we learn universal features [45], which are not asset-specific, then update the model for each asset class.

It was observed that rather than multi-head attention being an alternative to the changepoint detection (CPD) module, the two approaches actually work well in conjunction, leading to superior risk-adjusted returns. Furthermore, we found that multiple CPD timescales work well, with the Variable Selection approach helping to determine when a particular timescale is relevant. In particular, we found a combination of the one-month and biannual CPD timescales work the best.

We deconstruct our deep learning based momentum and mean-reversion strategy unlike any previous works. Our interpretable components help to shed light on how the model blends classical strategies based on the data. Looking at the interpretable attention patterns, we highlight the importance the model gives to significant events and how it segments the time-series into clearly defined regimes, learning regime-specific dynamics in the process. An interesting avenue for future work would be comparing this to Continual Learning, which is a paradigm whereby an agent sequentially learns new tasks.

VII. ACKNOWLEDGEMENTS

We would like to thank the Oxford-Man Institute of Quantitative Finance for financial and computing support.

REFERENCES

- [1] B. Lim, S. Zohren, and S. Roberts, “Enhancing time-series momentum strategies using deep neural networks,” *The Journal of Financial Data Science*, vol. 1, no. 4, pp. 19–38, 2019.
- [2] K. Wood, S. Roberts, and S. Zohren, “Slow momentum with fast reversion: A trading strategy using deep learning and changepoint detection,” *arXiv preprint arXiv:2105.13727*, 2021.
- [3] T. J. Moskowitz, Y. H. Ooi, and L. H. Pedersen, “Time series momentum,” *Journal of Financial Economics*, vol. 104, no. 2, pp. 228 – 250, 2012, Special Issue on Investor Sentiment.
- [4] W. F. Sharpe, “Capital asset prices: A theory of market equilibrium under conditions of risk,” *The Journal of Finance*, vol. 19, no. 3, pp. 425–442, 1964.
- [5] G. N. Bornholt, “The failure of the capital asset pricing model (CAPM): An update and discussion,” *Available at SSRN 2224400*, 2012.
- [6] B. Hurst, Y. H. Ooi, and L. H. Pedersen, “A century of evidence on trend-following investing,” *The Journal of Portfolio Management*, vol. 44, no. 1, pp. 15–29, 2017.
- [7] Y. Lempérière, C. Deremble, P. Seager, M. Potters, and J.-P. Bouchaud, “Two centuries of trend following,” *Journal of Investment Strategies*, vol. 3, no. 3, pp. 41–61, 2014.
- [8] J. Baz, N. Granger, C. R. Harvey, N. Le Roux, and S. Rattray, “Dissecting investment strategies in the cross section and time series,” *SSRN*, 2015. [Online]. Available: <https://ssrn.com/abstract=2695101>
- [9] N. Baltas and R. Kosowski, “Momentum strategies in futures markets and trend-following funds,” in *Paris December 2012 Finance Meeting EUROFIDAI-AFFI Paper*, 2013.
- [10] A. Levine and L. H. Pedersen, “Which trend is your friend,” *Financial Analysts Journal*, vol. 72, no. 3, 2016.
- [11] B. Bruder, T.-L. Dao, J.-C. Richard, and T. Roncalli, “Trend filtering methods for momentum strategies,” *SSRN*, 2013. [Online]. Available: <https://ssrn.com/abstract=2289097>
- [12] A. Y. Kim, Y. Tse, and J. K. Wald, “Time series momentum and volatility scaling,” *Journal of Financial Markets*, vol. 30, pp. 103 – 124, 2016.
- [13] N. Baltas and R. Kosowski, “Demystifying time-series momentum strategies: Volatility estimators, trading rules and pairwise correlations,” *SSRN*, 2017. [Online]. Available: <https://ssrn.com/abstract=2140091>
- [14] C. R. Harvey, E. Hoyle, R. Korgaonkar, S. Rattray, M. Sargaison, and O. van Hemert, “The impact of volatility targeting,” *SSRN*, 2018. [Online]. Available: <https://ssrn.com/abstract=3175538>
- [15] N. Jegadeesh and S. Titman, “Returns to buying winners and selling losers: Implications for stock market efficiency,” *The Journal of Finance*, vol. 48, no. 1, pp. 65–91, 1993.
- [16] S. Hochreiter and J. Schmidhuber, “Long short-term memory,” *Neural Computation*, vol. 9, no. 8, pp. 1735–1780, 1997.
- [17] Y. Bengio, P. Simard, and P. Frasconi, “Learning long-term dependencies with gradient descent is difficult,” *IEEE Transactions on Neural Networks*, vol. 5, no. 2, pp. 157–166, 1994.
- [18] I. Goodfellow, Y. Bengio, and A. Courville, *Deep Learning*. MIT Press, 2016, <http://www.deeplearningbook.org>.
- [19] W. F. De Bondt and R. Thaler, “Does the stock market overreact?” *The Journal of Finance*, vol. 40, no. 3, pp. 793–805, 1985.
- [20] J. M. Poterba and L. H. Summers, “Mean reversion in stock prices: Evidence and implications,” *Journal of Financial Economics*, vol. 22, no. 1, pp. 27–59, 1988.
- [21] N. Jegadeesh, “Seasonality in stock price mean reversion: Evidence from the US and the UK,” *The Journal of Finance*, vol. 46, no. 4, pp. 1427–1444, 1991.

[22] A. Garg, C. L. Goulding, C. R. Harvey, and M. Mazzoleni, “Momentum turning points,” *Available at SSRN 3489539*, 2021.

[23] B. Lim and S. Zohren, “Time series forecasting with deep learning: A survey,” *arXiv preprint arXiv:2004.13408*, 2020.

[24] C. E. Rasmussen, “Gaussian processes in machine learning,” in *Summer school on machine learning*. Springer, 2003, pp. 63–71.

[25] R. Garnett, M. A. Osborne, S. Reece, A. Rogers, and S. J. Roberts, “Sequential Bayesian prediction in the presence of changepoints and faults,” *The Computer Journal*, vol. 53, no. 9, pp. 1430–1446, 2010.

[26] D. Bahdanau, K. Cho, and Y. Bengio, “Neural machine translation by jointly learning to align and translate,” *arXiv preprint arXiv:1409.0473*, 2014.

[27] I. Sutskever, O. Vinyals, and Q. V. Le, “Sequence to sequence learning with neural networks,” in *Advances in Neural Information Processing Systems 27 (NeurIPS)*, 2014, pp. 3104–3112.

[28] A. Vaswani, N. Shazeer, N. Parmar, J. Uszkoreit, L. Jones, A. N. Gomez, L. Kaiser, and I. Polosukhin, “Attention is all you need,” *arXiv preprint arXiv:1706.03762*, 2017.

[29] T. Lin, Y. Wang, X. Liu, and X. Qiu, “A survey of Transformers,” *arXiv preprint arXiv:2106.04554*, 2021.

[30] D. Poh, B. Lim, S. Zohren, and S. Roberts, “Enhancing cross-sectional currency strategies by ranking refinement with Transformer-based architectures,” *arXiv preprint arXiv:2105.10019*, 2021.

[31] S. Li, X. Jin, Y. Xuan, X. Zhou, W. Chen, Y.-X. Wang, and X. Yan, “Enhancing the locality and breaking the memory bottleneck of Transformer on time series forecasting,” *Advances in Neural Information Processing Systems (NeurIPS)*, vol. 32, pp. 5243–5253, 2019.

[32] B. Lim, S. O. Arik, N. Loeff, and T. Pfister, “Temporal Fusion Transformers for interpretable multi-horizon time series forecasting,” *arXiv preprint arXiv:1912.09363*, 2019.

[33] H. Zhou, S. Zhang, J. Peng, S. Zhang, J. Li, H. Xiong, and W. Zhang, “Informer: Beyond efficient Transformer for long sequence time-series forecasting,” in *The Thirty-Fifth AAAI Conference on Artificial Intelligence, AAAI 2021, Virtual Conference*, vol. 35, no. 12. AAAI Press, 2021, pp. 11106–11115.

[34] M. T. Ribeiro, S. Singh, and C. Guestrin, “”Why should I trust you?” Explaining the predictions of any classifier,” in *Proceedings of the 22nd ACM SIGKDD International Conference on Knowledge Discovery and Data Mining*, 2016, pp. 1135–1144.

[35] S. M. Lundberg and S.-I. Lee, “A unified approach to interpreting model predictions,” in *Advances in Neural Information Processing Systems 27 (NeurIPS)*, 2017, pp. 4768–4777.

[36] M.-T. Luong, H. Pham, and C. D. Manning, “Effective approaches to attention-based neural machine translation,” *arXiv preprint arXiv:1508.04025*, 2015.

[37] K. He, X. Zhang, S. Ren, and J. Sun, “Deep residual learning for image recognition,” in *Proceedings of the IEEE Conference on Computer Vision and Pattern Recognition*, 2016, pp. 770–778.

[38] N. Srivastava, G. Hinton, A. Krizhevsky, I. Sutskever, and R. Salakhutdinov, “Dropout: A simple way to prevent neural networks from overfitting,” *Journal of Machine Learning Research*, vol. 15, pp. 1929–1958, 2014.

[39] S. Kullback and R. A. Leibler, “On information and sufficiency,” *The Annals of Mathematical Statistics*, vol. 22, no. 1, pp. 79–86, 1951.

[40] C. Guo and F. Berkhahn, “Entity embeddings of categorical variables,” *arXiv preprint arXiv:1604.06737*, 2016.

[41] Y. N. Dauphin, A. Fan, M. Auli, and D. Grangier, “Language modeling with gated convolutional networks,” in *International Conference on Machine Learning*. PMLR, 2017, pp. 933–941.

[42] D. Kingma and J. Ba, “Adam: A method for stochastic optimization,” in *International Conference on Learning Representations (ICLR)*, 2015.

[43] “Pinnacle Data Corp. CLC Database,” <https://pinnacledata2.com/clc.html>.

[44] Z. Zhang, S. Zohren, and S. Roberts, “Deep reinforcement learning for trading,” *The Journal of Financial Data Science*, vol. 2, no. 2, pp. 25–40, 2020.

[45] J. Sirignano and R. Cont, “Universal features of price formation in financial markets: perspectives from deep learning,” *Quantitative Finance*, vol. 19, no. 9, pp. 1449–1459, 2019.

[46] M. Abadi *et al.*, “TensorFlow: Large-scale machine learning on heterogeneous systems,” 2015, software available from tensorflow.org. [Online]. Available: <https://www.tensorflow.org/>

[47] A. Paszke, S. Gross, S. Chintala, G. Chanan, E. Yang, Z. DeVito, Z. Lin, A. Desmaison, L. Antiga, and A. Lerer, “Automatic differentiation in PyTorch,” in *Autodiff Workshop – Advances in Neural Information Processing (NeurIPS)*, 2017.

APPENDIX

A. Dataset Details

Exhibit 10: Portfolio assets

Identifier	Description	Test From
Commodities (CM)		
CC	COCOA	1995
DA	MILK III, composite	2000
GI	GOLDMAN SAKS C. I.	1995
JO	ORANGE JUICE	1995
KC	COFFEE	1995
KW	WHEAT, KC	1995
LB	LUMBER	1995
NR	ROUGH RICE	1995
SB	SUGAR #11	1995
ZA	PALLADIUM, electronic	1995
ZC	CORN, electronic	1995
ZF	FEEDER CATTLE, electronic	1995
ZG	GOLD, electronic	1995
ZH	HEATING OIL, electronic	1995
ZI	SILVER, electronic	1995
ZK	COPPER, electronic	1995
ZL	SOYBEAN OIL, electronic	1995
ZN	NATURAL GAS, electronic	1995
ZO	OATS, electronic	1995
ZP	PLATINUM, electronic	1995
ZR	ROUGH RICE, electronic	1995
ZT	LIVE CATTLE, electronic	1995
ZU	CRUDE OIL, electronic	1995
ZW	WHEAT, electronic	1995
ZZ	LEAN HOGS, electronic	1995
Equities (EQ)		
CA	CAC40 INDEX	2000
EN	NASDAQ, MINI	2005
ER	RUSSELL 2000, MINI	2005
ES	S&P 500, MINI	2000
LX	FTSE 100 INDEX	1995
MD	S&P 400 (Mini electronic)	1995
SC	S&P 500, composite	2000
SP	S&P 500, day session	1995
XU	DOW JONES EUROSTOXX50	2005
XX	DOW JONES STOXX 50	2005
YM	Mini Dow Jones (\$5.00)	2005
Fixed Income (FI)		
DT	EURO BOND (BUND)	1995
FB	T-NOTE, 5yr composite	1995
TY	T-NOTE, 10yr composite	1995
UB	EURO BOBL	2005
US	T-BONDS, composite	1995
Foreign Exchange (FX)		
AN	AUSTRALIAN \$\$, composite	1995
BN	BRITISH POUND, composite	1995
CN	CANADIAN \$\$, composite	1995
DX	US DOLLAR INDEX	1995
FN	EURO, composite	1995
JN	JAPANESE YEN, composite	1995
MP	MEXICAN PESO	2000
NK	NIKKEI INDEX	1995
SN	SWISS FRANC, composite	1995

All futures in our portfolio are listed in Exhibit 10 and have less than 10% of data missing. We winsorise our data by limiting it to be within 5 times its exponentially weighted moving (EWM) standard deviations from its EWM average, using a 252-day half-life. This helps to limit the impact of outliers. We only use an asset if there is enough data available in the validation set for one at least one LSTM sequence. We list the start date of the first out-of-sample training window in which we include a given asset in Exhibit 10.

B. Experiment Settings

We calibrate our model using the training data by optimising on the Sharpe loss function via minibatch Stochastic Gradient Descent (SGD), using the *Adam* optimiser. We list the fixed model parameters for each architecture in Exhibit 11. We keep the last 10% of the training data, for each asset, as a validation set. We implement random grid search, as an outer optimisation loop, to select the best hyperparameters, based on the validation set. The parameter search grid for each architecture is listed in Exhibit 12 and the number of search iterations is a fixed parameter. Rather than minimising validation loss, as in [1, 2], we maximise the entire diversified strategy Sharpe ratio of the validation set. This helps to both stabilise the variability between repeated experiments and additionally leads to small improvements in risk-adjusted performance. We implement early stopping, using the stopping patience listed for each architecture in Exhibit 11. Early stopping terminates training if there is no longer an increase in the Sharpe ratio of the validation set during this time period. Alternatively, we terminate training when the maximum number of epochs

The LSTM and TFT models were implemented via the Keras API in TensorFlow [46]. The other Transformer models were implemented in PyTorch [47] because the original implementations of the Informer and Convolutional Transformer were in this framework. We partition our training set into non-overlapping sequences for most architectures. The Transformer and Informer, however, benefited from training with overlapping sequences, where the subsequent sequence starts one time-step after the beginning of the previous sequence. We shuffled the order in which each sequence appears in an epoch.

Exhibit 11: Fixed Parameters

Parameters	LSTM	Transformer	Decoder-Only Transformer	Convolutional Transformer	Informer	Decoder-Only TFT
Sequence length	63	63	63	63	63	252
Δ train start time	63	1	63	63	1	252
No. epochs	300	50	300	300	50	300
Stopping patience	25	8	25	25	8	25
Search Iterations	50	20	50	50	20	50
Train/valid ratio	90%/10%	90%/10%	90%/10%	90%/10%	90%/10%	90%/10%

Exhibit 12: Hyperparameter Search Grid

Parameters	LSTM	Transformer	Decoder-Only Transformer	Convolutional Transformer	Informer	Decoder-Only TFT
Mini-batch size	64, 128, 256	512, 1024	64, 128	64, 128	512, 1024	32, 64, 128
Learning rate	$10^{-4}, 10^{-3}, 10^{-2}, 10^{-1}$	$10^{-4}, 10^{-3}$	$10^{-4}, 10^{-3}$	$10^{-4}, 10^{-3}$	$10^{-4}, 10^{-3}$	$10^{-4}, 10^{-3}, 10^{-2}, 10^{-1}$
Dropout	0.1, 0.2, 0.3, 0.4, 0.5	0.1, 0.2, 0.3, 0.4, 0.5	0.1, 0.2, 0.3, 0.4, 0.5	0.1, 0.2, 0.3, 0.4, 0.5	0.1, 0.2, 0.3, 0.4, 0.5	0.1, 0.2, 0.3, 0.4, 0.5
Max gradient norm	$10^{-2}, 10^0, 10^2, 10^{-1}$	$10^{-3}, 10^{-2}, 10^{-1}$	$10^{-3}, 10^{-2}, 10^{-1}$	$10^{-3}, 10^{-2}, 10^{-1}$	$10^{-3}, 10^{-2}, 10^{-1}$	$10^{-2}, 10^0, 10^2$
Hidden layer size	5, 10, 20, 40, 80, 160	-	-	-	-	5, 10, 20, 40, 80, 160
No. heads	-	2,4	2,4	2,4,8	2,4,8	4
No. layers	-	1, 2, 3	1, 2, 3	2, 3, 4	1, 2, 3	-
d_{model}	-	8, 16, 32, 64	8, 16, 32, 64	8, 16, 32, 64	8, 16, 32, 64	-
$d_{\text{hidden}}/d_{\text{model}}$	-	1, 2, 4, 8	1, 2, 4, 8	1, 2, 4, 8	1, 2, 4, 8	-
kernel size, k	-	-	-	1, 3, 6, 9	-	-

Details specific to each of the candidate architectures can be found in [28, 31, 33, 32] and further details of the implementation of DMNs can be found in [1, 2].